Electronic Supplementary Material (ESI) for Journal of Materials Chemistry A.

Supporting Information

Rapid Synthesis of Mesoporous Hollow $Ni_xCo_{3-x}(PO_4)_2$ Shells Showing Enhanced Electrocatalytic and Supercapacitor Performances

*Jingchao Zhang, Yong Yang, Zhicheng Zhang, Xiaobin Xu, Xun Wang**

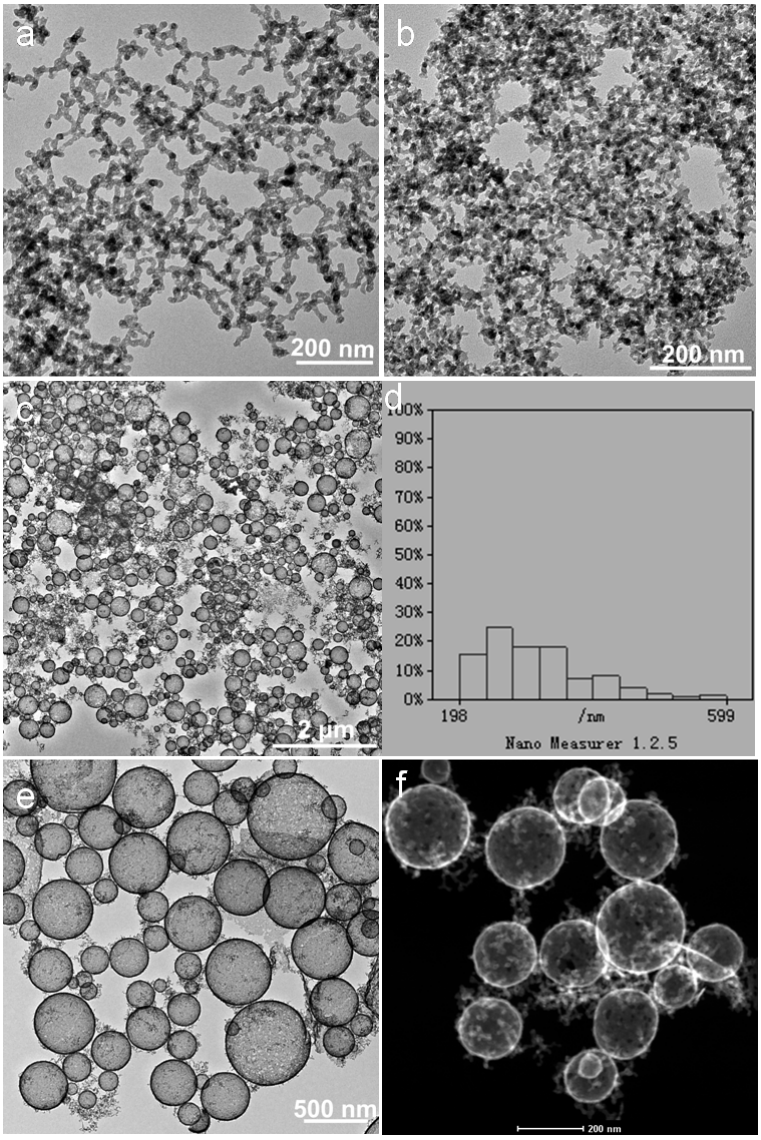

Fig. S1 (a) TEM images of the products with the absence of triethylamine and (b) with the absence of hexane in the synthesis system. (c) Low magnification TEM images. (d) Size distribution of $Co_3(PO_4)_2$ hollow shells from (c). (e) high magnification TEM image. (f) STEM image of the $Co_3(PO_4)_2$ hollow shells obtained by oil-in-water emulsions.

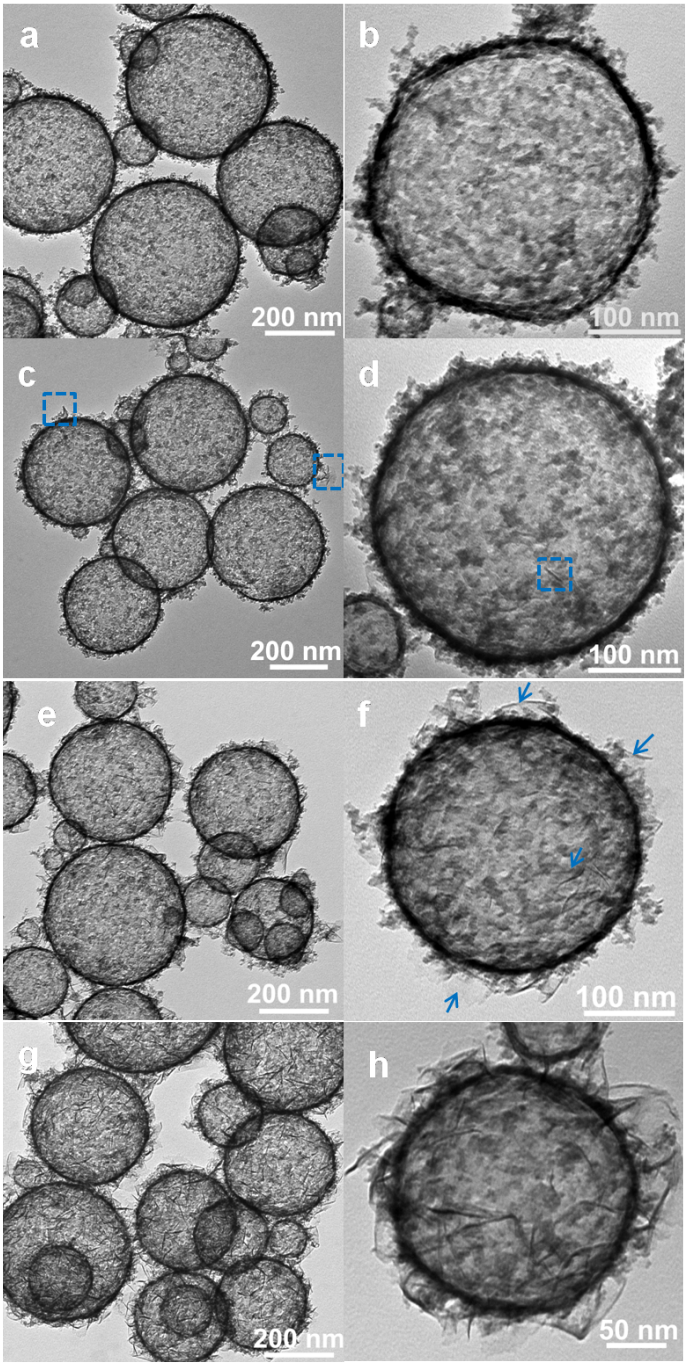

Fig. S2 TEM images of the $NiCo_2(PO_4)_2$ products obtained at 185 °C with microwave irradiation for different reaction time: (a-b) 1 min, (c-d) 5min, (e-f) 10 min, (g-h) 15 min.

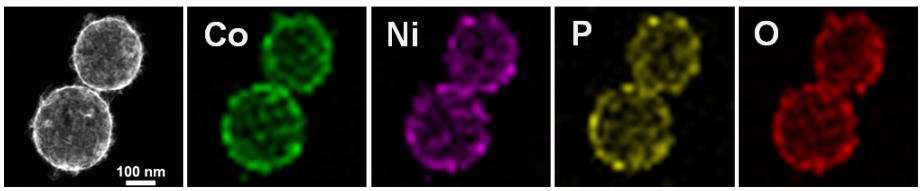

Fig. S3 STEM image and EDX elemental maps of the $NiCo_2(PO_4)_2$ hollow shells.

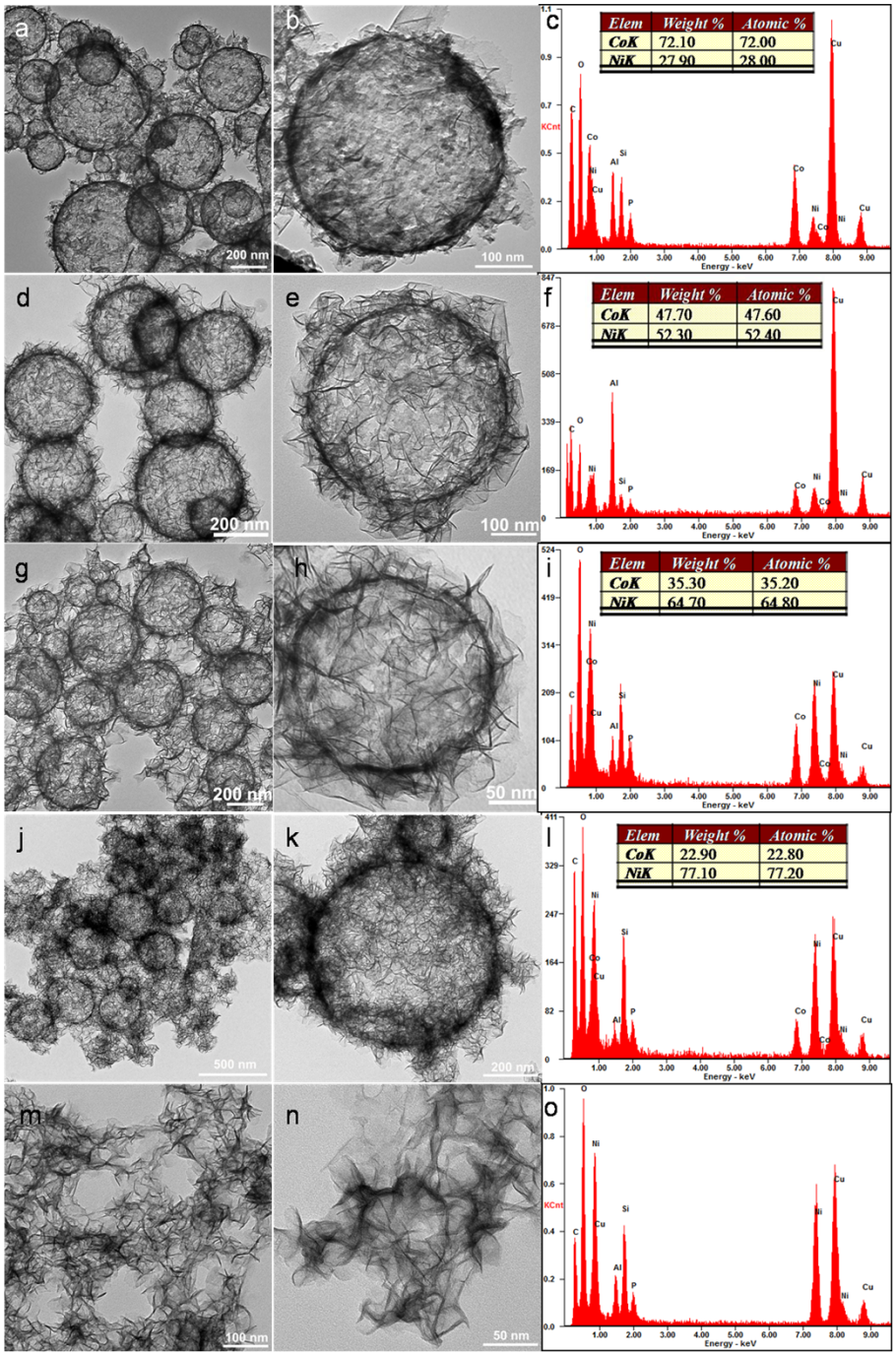

Fig. S4 TEM images and EDX spectra of the $Ni_xCo_{3-x}(PO_4)_2$ products obtained at 185 ^oC for 20 min with different molar ratios of Ni/Co: (a-c) mol (Ni/Co) = 1:3; (d-f) mol (Ni/Co) =1:1; (g-i) mol (Ni/Co) =2:1; (j-l) mol (Ni/Co) =3:1; and (m-o) mol (Ni/Co) = 3:0.

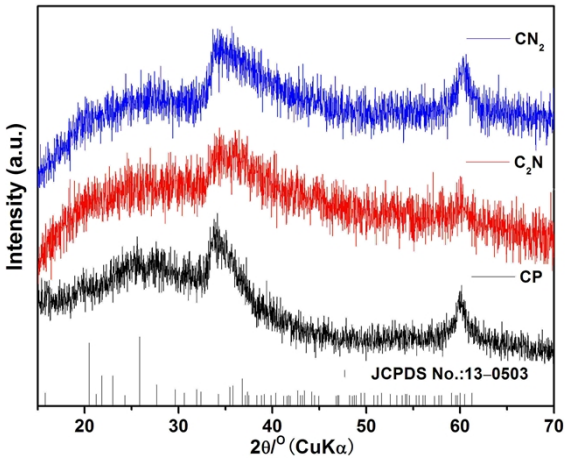

Fig. S5 (a) XRD patterns of the as-synthesized $Ni_xCo_{3-x}(PO_4)_2$ samples ($Co_3(PO_4)_2$, $NiCo_2(PO_4)_2$, and $CoNi_2(PO_4)_2$ was signed as CP, C_2N, and CN_2, respectively).

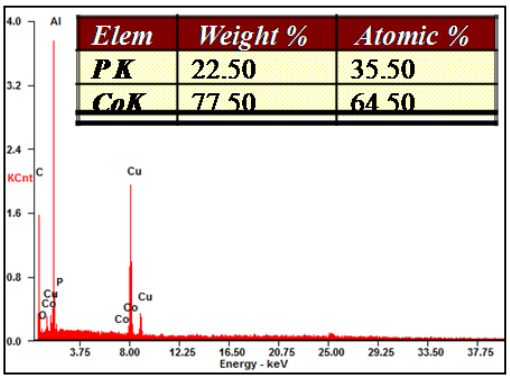

Fig. S6 EDX spectrum of the as-obtained $Co_3(PO_4)_2$ shells.

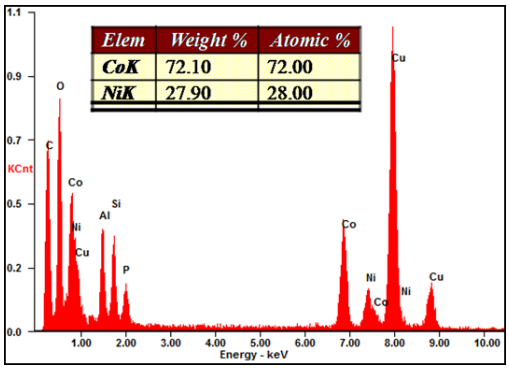

Fig. S7 EDX spectrum of the as-obtained $NiCo_2(PO_4)_2$ shells.

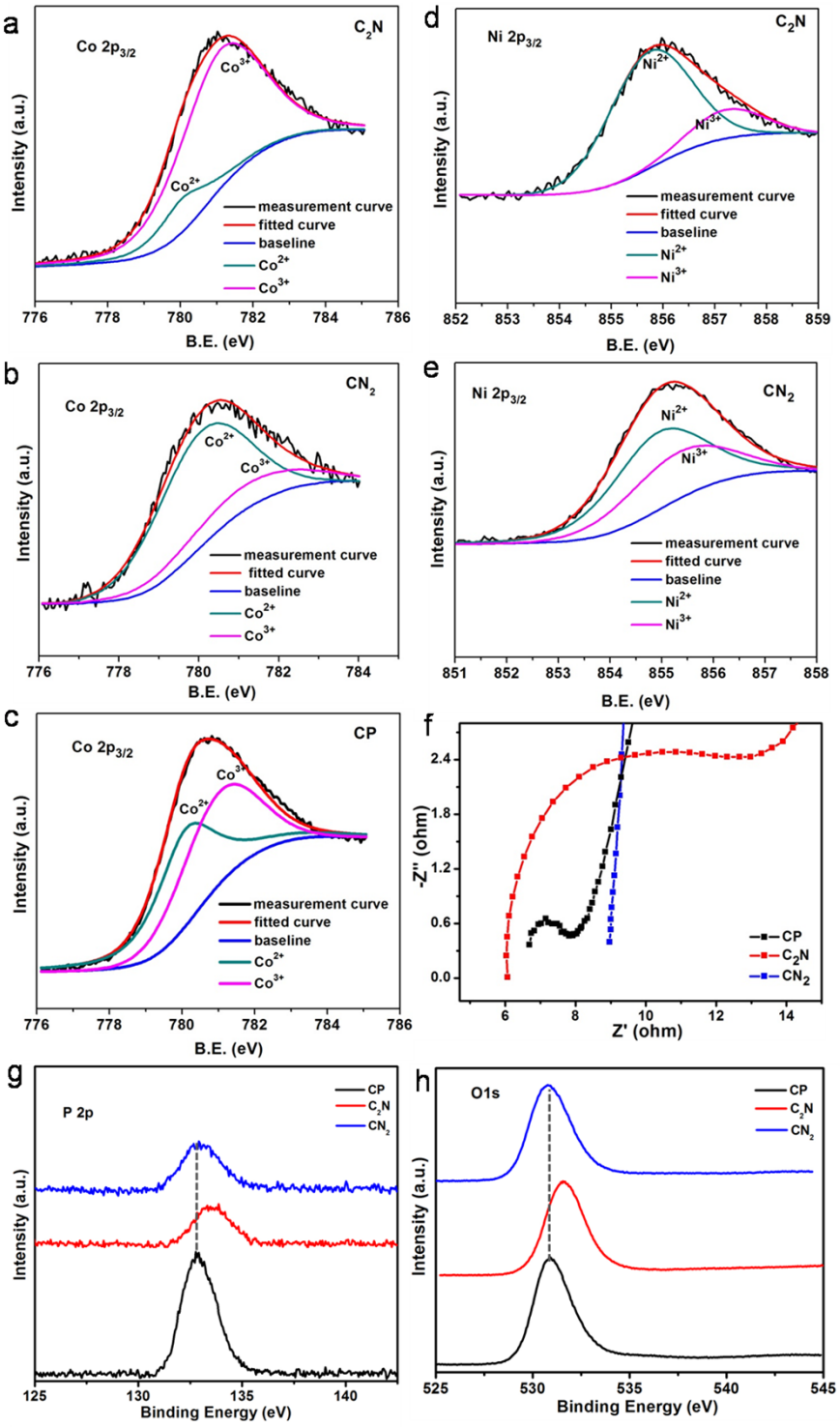

Fig. S8 (a-c) XPS spectra of Co 2p for the $NiCo_2(PO_4)_2$, $CoNi_2(PO_4)_2$, and $Co_3(PO_4)_2$ hollow shells. (d-e) Ni 2p for the $Co_2Ni(PO_4)_2$ and $CoNi_2(PO_4)_2$. (f) A magnified view of the high frequency region of the Nyquist impedance plots of the as-prepared $Co_3(PO_4)_2$, $NiCo_2(PO_4)_2$ and $CoNi_2(PO_4)_2$. (g-h) P 2p and O 1s for $Co_3(PO_4)_2$, $NiCo_2(PO_4)_2$, and $CoNi_2(PO_4)_2$.

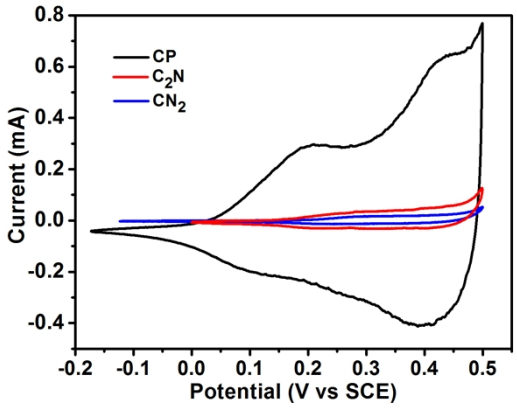

Fig. S9 Cyclic voltammetry curves of $Co_3(PO_4)_2$, $NiCo_2(PO_4)_2$ and $CoNi_2(PO_4)_2$ in 1M KOH (GCE, 5mm, 0.12mg/cm^2) conducted in static solution

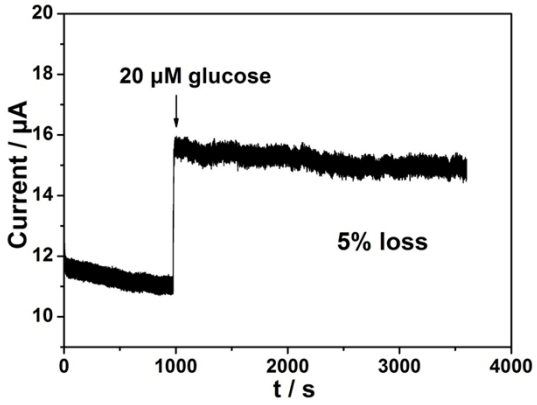

Fig. S10 Cycling stablization of amperometric sensing of glucose at the glucose concentration of 20 μM at $Co_3(PO_4)_2$/ GCE at 0.6 V in 0.1 M NaOH.

The specific capacitances derived from the discharge curves can be calculated from the following equation:

$$C=\frac{I\Delta t}{m\Delta V}$$

Where *I*, Δt, ΔV, and m was the discharging current (A), discharging time (s), discharging potential window (V), and mass of the electroactive material on the electrode (g), respectively.

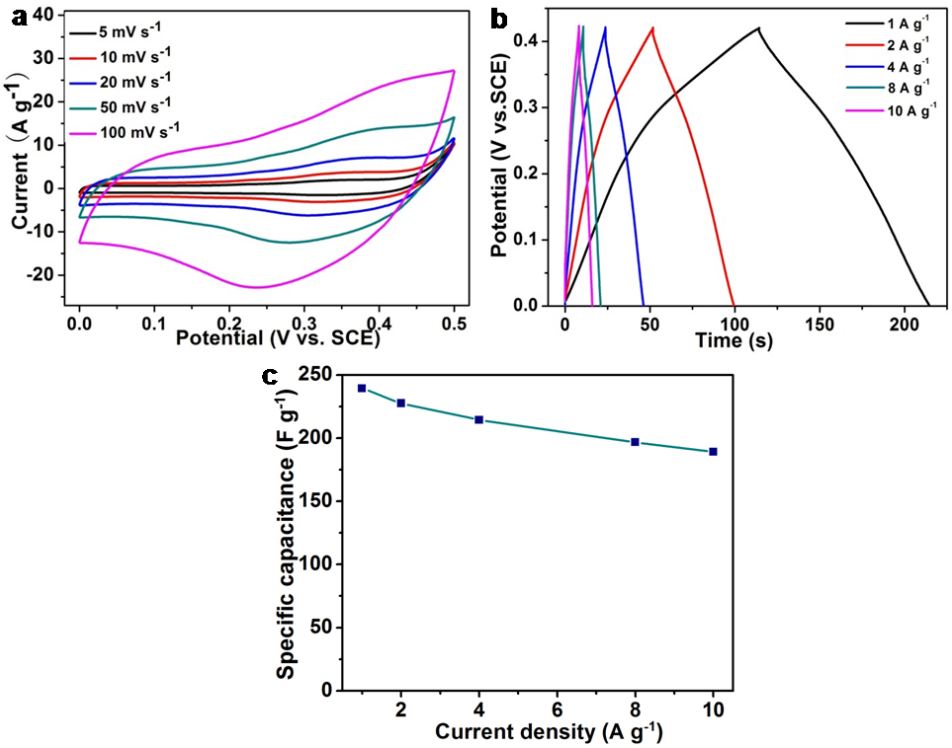

Fig. S11 (a) Cyclic voltammetry curves of mesoporous $Co_3(PO_4)_2$ shells modified electrode at various sweeping rates ranging from 5 to 100 mV s^{-1}. (b) Galvanostatic charge-discharge curves of $Co_3(PO_4)_2$ at different current densities. (c) Specific capacitance as a function of current density.

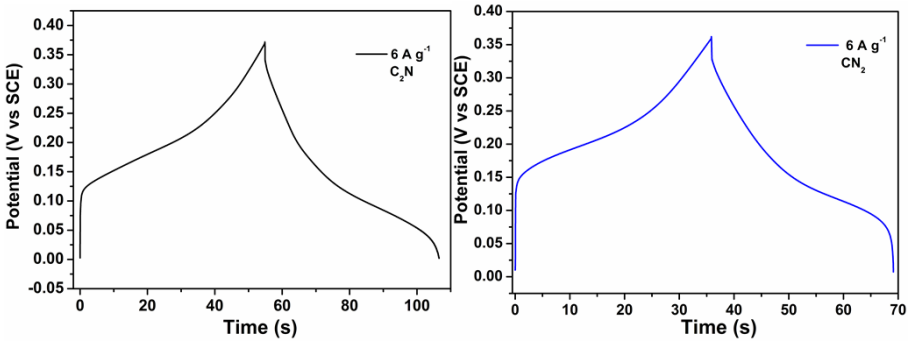

Fig. S12 Galvanostatic charge-discharge curves of $NiCo_2(PO_4)_2$ (C_2N)and $CoNi_2(PO_4)_2$ (CN_2) at 6A/g.

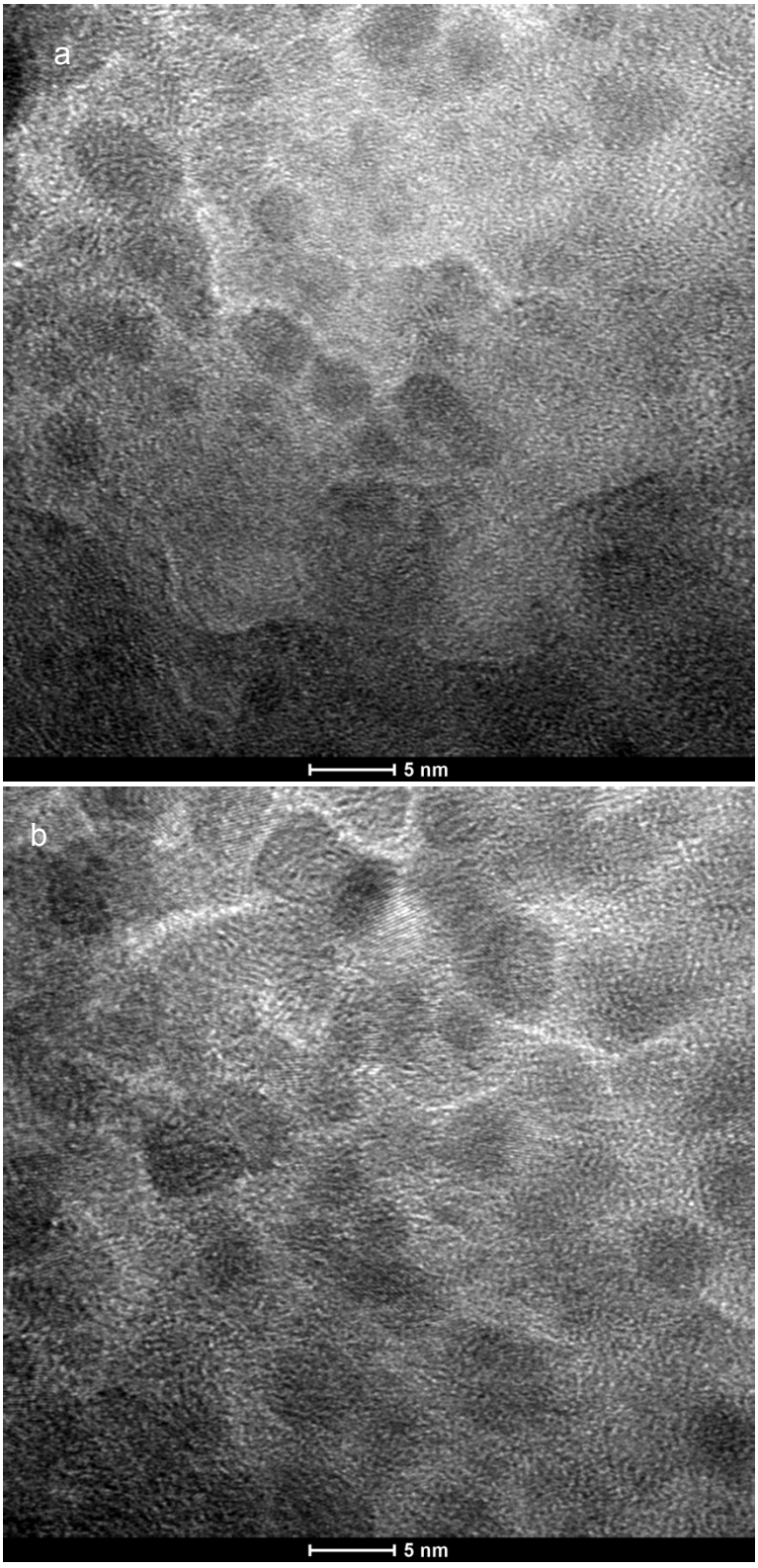
a
5 nm
b
5 nm

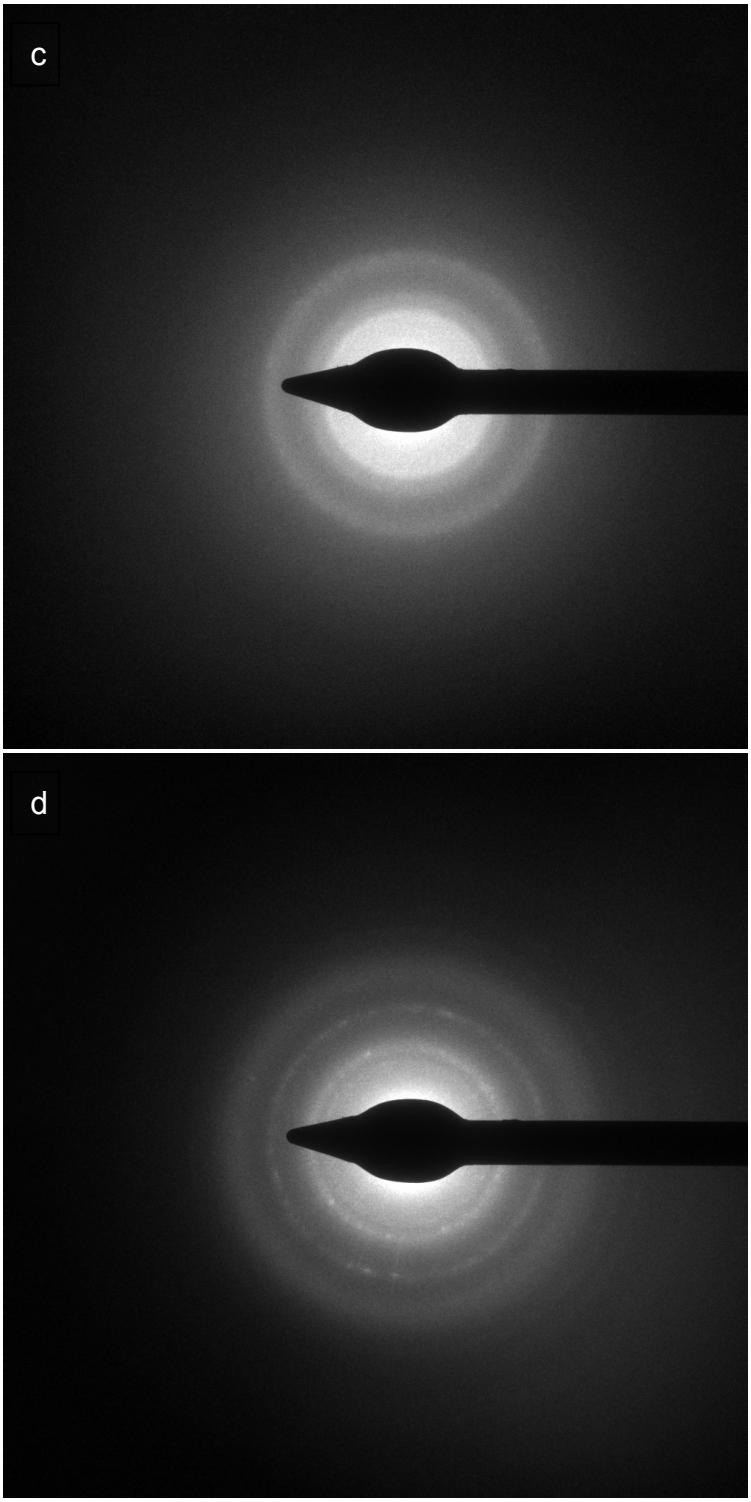

Fig. S13 HRTEM images of $Co_3(PO_4)_2$ sample irradiated by high energy electronic beam for a short (a) and long time (b). (c-d) The corresponding electron diffraction images of (a) and (b).